INTERNATIONAL JOURNAL OF OPTIMIZATION IN CIVIL ENGINEERING
Int. J. Optim. Civil Eng., 2017; 7(4): 579-596

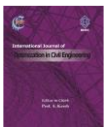

LINE-SEGMENTS CRITICAL SLIP SURFACE IN EARTH SLOPES USING AN OPTIMIZATION METHOD

M. Hajiazizi[1,*†], F. Heydari and M. Shahlaei
Department of Civil Engineering, Razi University, Taq-e Bostan, Kermanshah, Iran

ABSTRACT

In this paper the factor of safety (FS) and critical line-segments slip surface obtained by the Alternating Variable Local Gradient (AVLG) optimization method was presented as a new topic in 2D. Results revealed that the percentage of reduction in the FS obtained by switching from a circular shape to line segments was higher with the AVLG method than other methods. The 2D-AVLG optimization method is a new topic for finding critical line-segments slip surface which has been addressed in this paper. In fact, the line-segments slip surface is a flexible slip surface. Examples proves the efficiency and precision of the 2D-AVLG method for obtaining the line-segments critical slip surface compared to the circular and circular-line slip surfaces.

Keywords: line-segments; critical slip surface; optimization method; earth slope; 2D analysis.

Received: 20 February 2017; Accepted: 19 April 2017

1. INTRODUCTION

In slope stability analysis the slip surface is assumed to be a circular shape in many methods. Although in homogeneous soils the slip surface of line-segments is more realistic than circular slip surfaces, application of the slip surface of line-segments is necessary with non-homogeneous multilayer soils as the circular slip surface is not satisfactorily reliable. However, the shape of the slip surface has shown that might be a non-circular shape using numerical methods. It should be noted that numerical methods unable to locate the slip surface, exactly. It is worth mentioning that the slip surface of line-segments is more likely to comply with natural slip surfaces.

Bolton et al. [1] described the use of a global optimization algorithm for determining the critical failure surface in slope stability analyses. They concluded that the solution was

[*]Corresponding author: Department of Civil Engineering, Razi University, Taq-e Bostan, Kermanshah, Iran
[†]E-mail address: mhazizi@razi.ac.ir (M. Hajiazizi)

completely general. Jade and Shanker [2] proposed a modelling of slope failure of natural slopes using the RST-2 algorithm, a random search global optimization technique. Optimization techniques have been shown to be the most efficient means, for locating non-circular slip surfaces [3-7]. AVLG method is an approach in optimization process and it is based on the Univariate method [8]. It is a new approach to the optimization of line-segments slip surface in slope stability analysis. Factor of safety is a non-linear programing type, non-convex, and non-smooth objective function [9]. Li and White [10] and Celestino and Duncan [11] described Alternating Variable method for determining of critical slip surface. Baker [12] presented the Dynamic Programming method for determining of critical slip surface. Also, the critical slip surface determined by Arai and Tagyo [3] using the Conjugate- Gradient method, Malkawi et al. [5] using the Monte Carlo method, Chun and Chameau [13] using the Simplex method and Chen and Shao [14] and Chen [15] using the Random Generation method. Liu et al. [16] presented a comparison between the factor of safety resulted from the limit equilibrium method (LEM) for circular and circle-line slip surfaces and the factor of safety resulted from the enhanced limit slope stability (ELS) and shear strength reduction (SR) methods for non-circular slip surfaces. It is worth mentioning that the geometrical positions of slip surfaces resulted from ELS and SR methods can't be determined precisely. Hajiazizi and Tavana [17] used an optimization method for 3D slope stability. Sometimes, the circle-line slip surface is unrealistic similar to Fig. 1 in the article by Liu et al. [16], where a nonrealistic slip surface was obtained by changing the Poisson coefficient to 0.3. In other words, line-segments slip surfaces, which are properly flexible, could lead to slip surfaces that match the natural slip surfaces. Pina and Jimenez [18] proposed a new genetic algorithm (GA) that produce kinematically feasible slip surfaces with a high probability. Kang et al. [19] proposed an artificial bee colony algorithm with a multi-slice adjustment method for locating the critical slip surfaces of soil slopes, and the Spencer method employed to calculate the factor of safety.

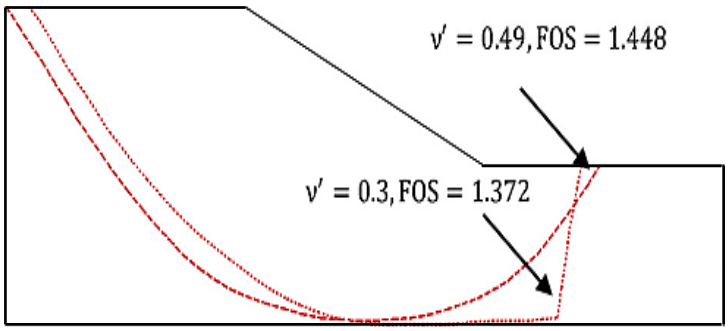

Figure 1. The circle-line slip surface is unrealistic with FS=1.372 [16]

Nowadays, the more importance of application of optimization methods in engineering area such as civil engineering, mechanical engineering, chemical engineering, electrical engineering has been considered [20- 23]. This paper deals with the development and implementation of the 2D-AVLG method in the analysis of slope stability using line-segments slip surface and a comparison of the line-segments slip surface and the circular and circular-line slip surfaces in earth slopes published by Liu et al. [16]. DOSS program [24]

was written by authors for obtaining the circular critical slip surfaces and line-segments critical slip surface that is more consistent with the actual slip surface in the nature. Finally, the results of this program will be compared with those obtained from LEM and two finite element methods (ELSM and SRM) published by Liu et al. [16].

2. 2D ALTERNATING VARIABLE LOCAL GRADIENT METHOD

The AVLG method is based on the theory of the Univariate method. The Univariate method is described as follows [8]:

1. Select an arbitrary starting point $\boldsymbol{X}_i$ and set $i = 1$
2. Find the search direction $\boldsymbol{S}_i$

$$\boldsymbol{S}_i^T = \begin{cases} (1,0,0,\dots,0) & \text{for} \quad i = 1, n+1, 2n+1, \dots \\ (0,1,0,\dots,0) & \text{for} \quad i = 2, n+2, 2n+2, \dots \\ (0,0,1,\dots,0) & \text{for} \quad i = 3, n+3, 2n+3, \dots \\ \vdots & \\ (0,0,0,\dots,1) & \text{for} \quad i = n, 2n, 3n, \dots \end{cases} \tag{1}$$

3. Find the optimal step length λ_i^* that

$$f(\boldsymbol{X}_i \pm \lambda_i^* \boldsymbol{S}_i) = min(\boldsymbol{X}_i \pm \lambda_i \boldsymbol{S}_i) \tag{2}$$

4. Consider $X_{i+1} = X_i \pm \lambda_i^* S_i$, depending on the direction for decreasing the value f, and fi+1=f(Xi+1)
5. Consider the new value of $i = i + 1$ and repeat from step 2.

For finding the most critical line-segments slip surface the AVLG method in 2D can be described as follows:

1. Set i=1
2. Finding the circular critical slip surface and taking it as the initial slip surface.
3. Selecting the suitable nodes on the circular critical slip surface and connecting them to each other. Zi denotes the coordinates of the initial nodes.

$$\boldsymbol{Z}_i = (x_1, y_1, x_2, y_2, \dots, x_n, y_n) \tag{3}$$

4. The best location for the first node on the slope boundary.
   The new coordinates of slip surface are:

$$\boldsymbol{Z}_i^* = (x_1^*, y_1^*, x_2, y_2, \dots, x_n, y_n) \tag{4}$$

5. The best location for the next node while also keeping the other nodes fixed results in a lower factor of safety. The best location for each internal node is obtained by its moving in the negative direction of the local gradient vector. The equation for the negative direction of the local gradient vector is:

$$\boldsymbol{S}_k = -\boldsymbol{G}_k = -\left\{\frac{\partial Fs}{\partial x_k}, \frac{\partial Fs}{\partial y_k}\right\}^T \tag{5}$$

where, the new coordinates of the slip surface are:

$$\boldsymbol{Z}_i^* = (x_1^*, y_1^*, x_2^*, y_2^*, x_3, y_3, \dots, x_n, y_n) \tag{6}$$

6. Find the best location for the subsequent internal node while other nodes remain fixed. This process is iterated for the rest of the internal nodes. The new coordinates of the slip surface are as follows:

$$\boldsymbol{Z}_i^* = (x_1^*, y_1^*, x_2^*, y_2^*, \dots, x_k^*, y_k^*, \dots, x_n, y_n) \tag{7}$$

7. Finding the best location for the last node which the first optimization cycle is terminated. The new coordinates of the slip surface are:

$$\boldsymbol{Z}_{i+1}^* = (x_1^*, y_1^*, x_2^*, y_2^*, \dots, x_{n-1}^*, y_{n-1}^*, x_n^*, y_n^*) \tag{8}$$

8. Set i=i+1
9. Steps 4 to 7 are repeated for several cycles and new coordinates are obtained until the difference between the safety factors of the last two cycles is less than ε=1×10-5. Or

$$|FS(\mathbf{Z}_{i+1}^*) - FS(\mathbf{Z}_i^*)| < \varepsilon \tag{9}$$

FS ($\mathbf{Z}^*_{i+1}$) = for the last optimization cycle,
FS ($\mathbf{Z}^*_i$) = for the penultimate optimization cycle.
FS ($\mathbf{Z}^*_{i+1}$) is taken as the most critical slip surface.

3. SLOPE STABILITY ANALYSIS METHODS

The slope stability analysis is a statically indeterminate problem, and there are different methods of analysis available to the designer. Slope stability analysis can be carried out by using the limit equilibrium method (LEM), the limit analysis method (LAM) and numerical methods (NMs). The factor of safety for slope stability analysis is usually defined from the shear strength to the shear stress ratio at a given failure. There are several ways in formulating the factor of safety.

3.1 Limit equilibrium method

The limit equilibrium method is an approach in slope stability analysis. This method, statically is an indeterminate problem, and assumptions on the inter-slice shear forces are required to change to statically a determinate problem. Based on the assumptions there are more than ten methods developed for slope stability analysis, such as the Fellenius method, the Bishop simplified, Spencer, and Morgenstern-Price methods [7].

In the conventional limiting equilibrium method, the shear stress τ_m which can be mobilized along the failure surface is given by:

$$\tau_m = \tau_f / FS \tag{10}$$

where FS is the factor of safety, τ_f is shear strength as follows,

$$\tau_f = c' + \acute{\sigma_n} \tan \acute{\phi} \tag{11}$$

where c' is the effective cohesion, σ'_n is the effective normal stress, φ' is the angle of effective internal friction.

In briefly the LEM formulation is written as follows:

$$FS = \frac{shear\ stregth\ on\ a\ given\ slip\ surface}{shear\ stress\ on\ a\ given\ slip\ surface} \tag{12}$$

Eq. (12) can also be written as follows:

$$\tau_i = \frac{\tau_{fi}}{FS} = \frac{c' + \sigma'_i \tan \acute{\varphi}}{FS} = \frac{c'}{FS} + \sigma'_i \frac{\tan \varphi'}{FS} \tag{13}$$

Conventionally, the critical slip surface for a given slope is estimated by comparing safety factors of several trial slip surfaces. Among all trial slip surfaces, the slip surface that has the lowest factor of safety is selected as the critical failure surface. Several optimization approaches by using LEM have been employed to automate the search for the critical failure surface [3-6].

3.1.1 The objective function for optimization

The objective function of the factor of safety is nonlinear non-smooth. Then the search for global critical slip surface of soil slope is difficult as the objective function of the safety factor. The objective function for optimization is,

$$\mathrm{FS} = f_0 \frac{1}{\sum_{i=1}^{n} \mathrm{W}_i \tan \alpha_i} \sum_{i=1}^{n} \left\{ \mathrm{C}' \Delta x_i + (\Delta \mathrm{W}_i - \mathrm{u}_i \Delta x_i) \tan \phi_i' \right\} \left\{ \frac{\sec^2 \alpha_i}{1 + \tan \alpha_i \frac{\tan \phi_i'}{\mathrm{FS}}} \right\} \tag{14}$$

Or

$$\mathrm{FS} = f_0 \sum \mathrm{F}_i / \sum G_i \tag{15}$$

where

$$F_i = \frac{C_i \Delta x + (\Delta w_i - u\Delta x_i)\tan\phi_i}{1 + \frac{\tan\alpha_i \tan\phi_i}{FS}}(1+\tan^2\alpha_i) \tag{16}$$

$$G_i = \Delta w_i \tan\alpha_i \tag{17}$$

$$\Delta w_i = \{(f_i - y_i) + (f_{i+1} - y_{i+1})\}(x_{i+1} - x_i)^{\gamma}/_2 \tag{18}$$

$$\tan\alpha_i = (y_{i+1} - y_i)/(x_{i+1} - x_i) \tag{20}$$

This optimization problem cannot be solved directly, because the right-hand side of Eq. 14 includes FS. Here the following numerical graphical method is employed. In the numerical graphical solution scheme, the optimization problem is solved provisionally for an assumed value of FS in the right-hand side Eq. 14 and a plot is made in a way shown in Fig. 2. Repetition of this operation yields curves, which specify the relation between two FS. The point of intersection between the curve and the straight line with unit gradient such as in Fig. 2 gives a solution of this problem.

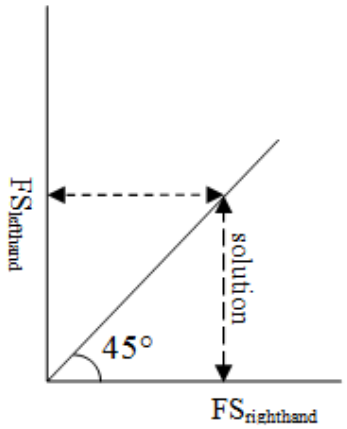

Figure 2. Numerical graphical solution scheme

The gradient of the objective function FS on x_i and y_i are calculated as,

$$\frac{\partial FS}{\partial x_i} = \left\{(\partial\sum_{j=1}^{n} F_j / \partial x_i)\sum_{j=1}^{n} G_j - \sum_{j=1}^{n} F_j(\partial\sum_{j=1}^{n} G_j / \partial x_i)\right\}/(\sum_{j=1}^{n} G_j)^2 \tag{20}$$

and

$$\frac{\partial FS}{\partial y_i} = \left\{(\partial\sum_{j=1}^{n} F_j / \partial y_i)\sum_{j=1}^{n} G_j - \sum_{j=1}^{n} F_j(\partial\sum_{j=1}^{n} G_j / \partial y_i)\right\}/(\sum_{j=1}^{n} G_j)^2 \tag{21}$$

where,

$$\partial\sum_{j=1}^{n} \mathrm{F}_j / \partial x_i = \partial \mathrm{F}_i / \partial x_i + \partial \mathrm{F}_{i-1} / \partial x_i \tag{22}$$

$$\partial\sum_{j=1}^{n} \mathrm{F}_j / \partial y_i = \partial \mathrm{F}_i / \partial y_i + \partial \mathrm{F}_{i-1} / \partial y_i \tag{23}$$

$$\partial\sum_{j=1}^{n} \mathrm{G}_j / \partial x_i = \partial \mathrm{G}_i / \partial x_i + \partial \mathrm{G}_{i-1} / \partial x_i \tag{24}$$

$$\partial\sum_{j=1}^{n} \mathrm{G}_j / \partial y_i = \partial \mathrm{G}_i / \partial y_i + \partial \mathrm{G}_{i-1} / \partial y_i \tag{25}$$

$$\frac{\partial \mathrm{F}_i}{\partial y_i} = [-\left\{0.5\,\gamma \tan\phi_i \Delta x_i \ \mathrm{FS}(1+\tan^2\alpha_i) + (\mathrm{C}'_{\mathrm{i}} + \frac{\mathrm{W}_i \tan\phi_i}{\Delta x_i})\mathrm{FS}\,2\tan\alpha_i\right\}$$
$$\times(\mathrm{FS}+\tan\alpha_i \tan\phi_i) + (\mathrm{C}'_i + \frac{\mathrm{W}_i \tan\phi_i}{\Delta x_i})\mathrm{FS}(1+\tan^2\alpha_i)\tan\phi_i] \tag{26}$$
$$/(\mathrm{FS}+\tan\alpha_i \tan\phi_i)^2 \tag{26}$$

$$\frac{\partial \mathrm{F}_{i-1}}{\partial y_i} = [-\left\{0.5\,\gamma \tan\phi_i \Delta x_{i-1} \ \mathrm{FS}(1+\tan^2\alpha_{i-1}) + (\mathrm{C}'_{\mathrm{i}} + \frac{\mathrm{W}_{i-1} \tan\phi_{i-1}}{\Delta x_{i-1}})\mathrm{FS}\,2\tan\alpha_{i-1}\right\}$$
$$\times(\mathrm{FS}+\tan\alpha_{i-1} \tan\phi_i) + (\mathrm{C}'_i + \frac{\mathrm{W}_{i-1} \tan\phi_{i-1}}{\Delta x_{i-1}})\mathrm{FS}(1+\tan^2\alpha_{i-1})\tan\phi_i] \tag{27}$$
$$/(\mathrm{FS}+\tan\alpha_{i-1} \tan\phi_i)^2$$

$$\partial \mathrm{G}_i / \partial x_i = 0 \tag{28}$$

$$\partial \mathrm{G}_i / \partial y_i = 0.5\,\gamma\,(2y_i - f_i - f_{i+1}) \tag{29}$$

$$\partial \mathrm{G}_{i-1} / \partial x_i = 0 \tag{30}$$

$$\partial \mathrm{G}_{i-1} / \partial y_i = 0.5\,\gamma\,(f_{i-1} + f_i - 2y_i) \tag{31}$$

The partial derivatives of a function FS, with respect to each of the 2n variables are collectively called the gradient of the function and is denoted by ∇FS,

$$\underset{2n\times 1}{\nabla \mathrm{FS}} = \begin{Bmatrix} \partial \mathrm{FS}/\partial x_1 \\ \partial \mathrm{FS}/\partial y_1 \\ \vdots \\ \partial \mathrm{FS}/\partial x_n \\ \partial \mathrm{FS}/\partial y_n \end{Bmatrix} \tag{32}$$

3.2 Shear strength reduction method (SRM)

In the SRM, the gravity load vector for a material with unit weight γ_s is determined from Eq. (33) as follows [25]:

$$\{f\} = \gamma_s \int [N]^T dv \tag{33}$$

where {f} is the equivalent body force vector and $[N]$ is the shape factor matrix. The material parameters c' and φ' are reduced according to

$$c'_f = \frac{c'}{FS}; \qquad \varphi'_f = arc\tan\{\tan(\varphi'/FS)\} \tag{34}$$

The factor of safety FS keeps on changing until the ultimate state of the system is attained, and the corresponding factor of safety will be the factor of safety of the slope [25].

The location of the critical failure surface is usually determined from the contour of the maximum shear strain or the maximum shear strain rate. SRM can give, movements and pore pressures which are not possible with the LEM. However, the SRM unable to locate the slip surface, exactly.

3.3 Enhanced limit slope stability (ELS) method

In the ELS method, the FS can be obtained as:

$$FS = \frac{\sum_{i=1}^{n} \tau_{fi} \Delta L_i}{\sum_{i=1}^{n} \tau_i \Delta L_i} = \frac{\int \tau_f dl}{\int \tau dl} \tag{35}$$

where n=the number of discrete segments along L, ΔLi=the length of segment i. The primary task of the ELS method is to locate the critical slip surface using mathematical optimization [16].

4. EXAMPLES

To investigate the differences and compare the results of the AVLG method (line-segments slip surface), LEM, SRM and ELSM (circular and line-circular slip surface), four examples were selected from [16]. These examples have been widely used in the engineering literature. In this article, the values of factor of safety and slip surfaces were calculated and compared using the four aforementioned methods.

4.1 Example 1

The inclined surface studied in this example is depicted in Fig. 3. The embankment height is equal to 5m and $C_{u1}/\gamma H = 0.25$. Table 1 shows the soil characteristics for two layers in Fig. 3. Fig. 4 compares the critical slip surfaces resulted from the limit equilibrium, the strength reduction, and ELS methods. This figure was prepared by [16]. Fig. 5 shows the circular and line-segment critical slip surfaces resulted from the AVLG method for case1 and case2. [16] indicated that the FS resulted from ELS method was close to the FS resulted from SRM. In Table 2, the FS obtained from LEM1 is larger than those obtained from the two finite element methods, which could be explained by the assumed circular arc slip surface. The FS

obtained from LEM3 is the smallest; however, the corresponding non-circular critical slip surface is extremely different from those obtained from the two finite element methods. As seen in Table 2, the FS of the non-circular slip surfaces is smaller than the FS of the circular slip surface. The percentage of reduction in FS using AVLG in case1 was 7.9, which was the maximum level of reduction attainable. This reduction reflects the flexibility and efficiency of the AVLG method in finding the most critical slip surface. In case2, the reduction by the AVLG method was also satisfactory. Although the reduction was lower than the LEM3 (C-optimized) method, the difference was not significant.

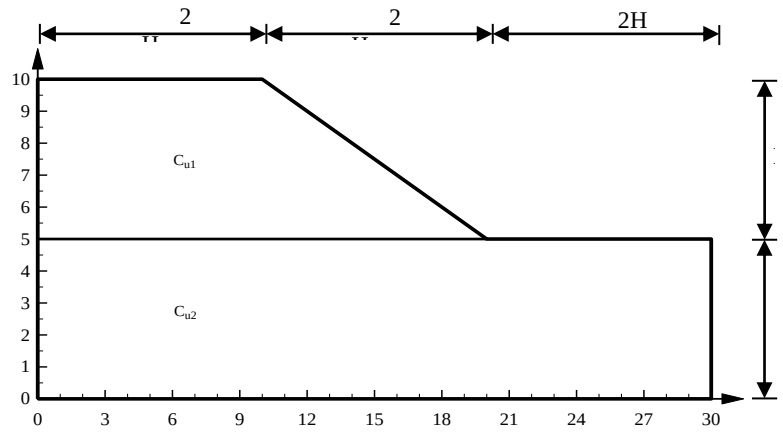

Figure 3. A clay slope with a weak foundation layer

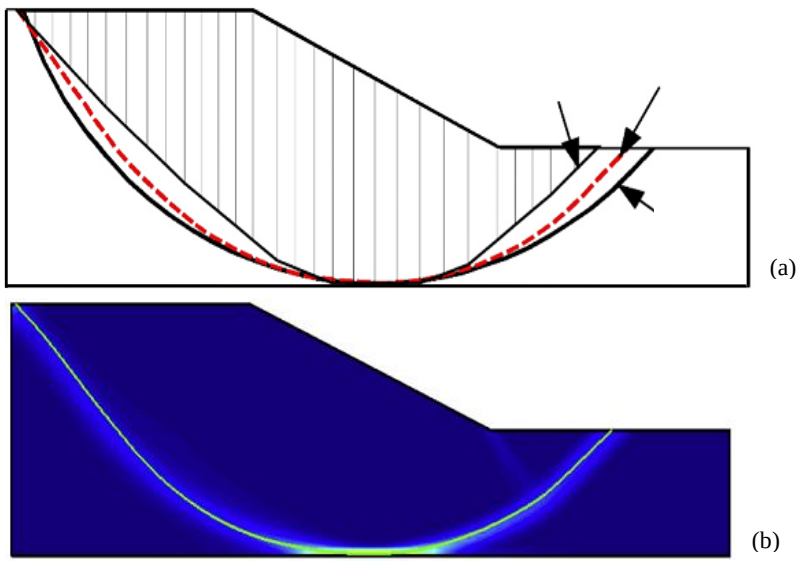

Figure 4. Comparisons of the critical slip surfaces obtained from (a) the LEM (solid lines) And ELSM (dashed line) and (b) the SRM for case1 [16]

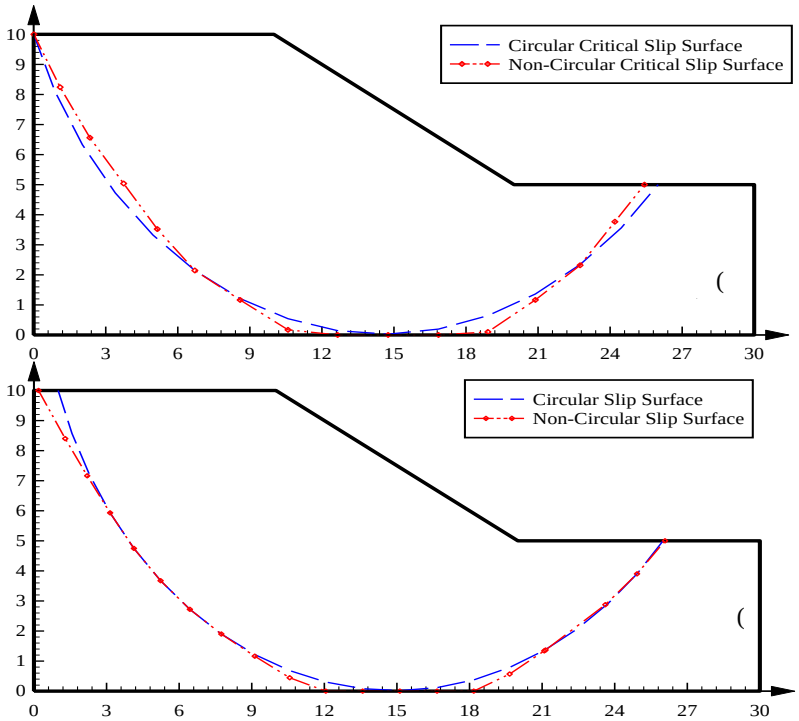

Figure 5. Comparison between initial and optimization slip surfaces with DOSS software (a) case1, (b) case2 (this study)

Table 1: Geotechnical parameters for example 1

Case	$\gamma(kN/m^3)$	$c_{u2}/c_{u1}\ (-)$	$E(kN/m^2)$	$\vartheta(-)$
1	20.0	1.0	10^5	0.49
2	20.0	0.8	10^5	0.49

Table 2: Factors of safety for example1

Method	**Case1**	**FS** difference with Circular slip surface	**Case2**	**FS** difference with Circular slip surface
LEM1(A-circular) [16]	1.474		1.235	
LEM2(B-fully specified) [16]	1.455	1.3	1.202	2.7
LEM3(C-optimized) [16]	1.362	7.6	1.120	9.3
SRM(Coarse mesh) [16]	1.460	0.95	1.210	2
SRM(fine mesh) [16]	1.451	1.6	1.215	1.6
ELSM [16]	1.448	1.7	1.211	1.9
AVLG(LEM-critical circular slip surface)[this study]	1.440		1.230	
AVLG(critical line-segments slip surface)[this study]	1.326	7.9	1.116	9.2

4.2 Example 2

In this example, a homogeneous soil slope with a slope height equal to H=5 m, slope angle equal to 25.67° and $\acute{c}/\gamma H = 0.05$ is considered (Fig. 6). The soil characteristics show in Table 3. The critical slip surfaces from the two finite element methods and the limit equilibrium method (Fig. 7) and AVLG method (Fig. 8) are in good agreement. As seen in Table 4, the non-circular slip surfaces of SRM and ELS method resulted in larger factors of safety as compared to the circular slip surfaces obtained by [16]. The values of critical line-segments and circular FS resulted from the AVLG method were 1.166 and 1.35, respectively. The 13.6% reduction in FS values reflected the effectiveness of the line-segment slip surface to find smaller factors of safety.

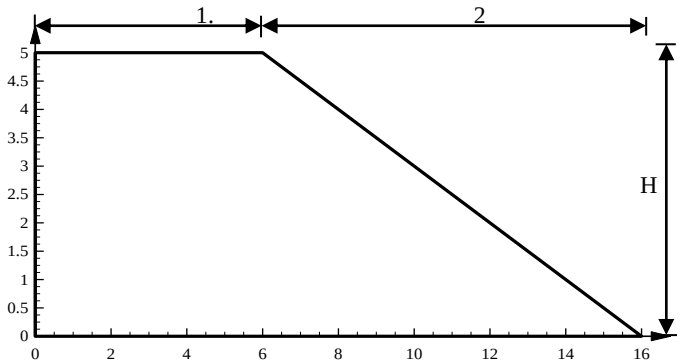

Figure 6. A homogeneous slope with a slope angle of 25.67° (2:1), $c/\gamma H = 0.05$

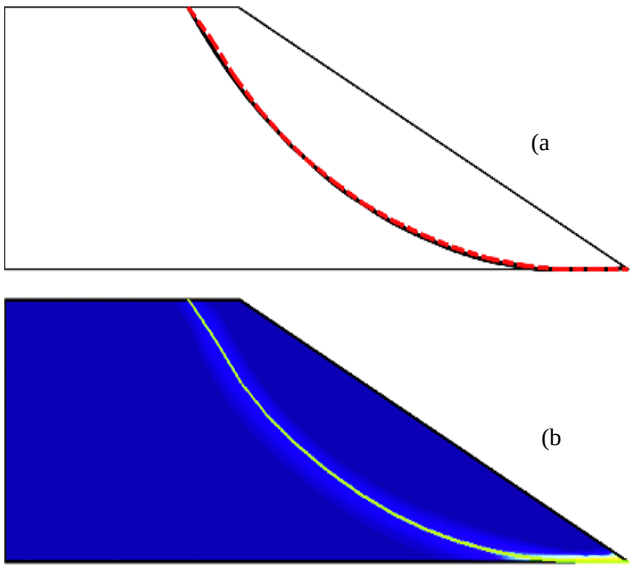

Figure 7. Comparisons of the critical slip surfaces obtained from (a) the LEM (solid line) and ELSM (dashed line) (b) the SRM [16]

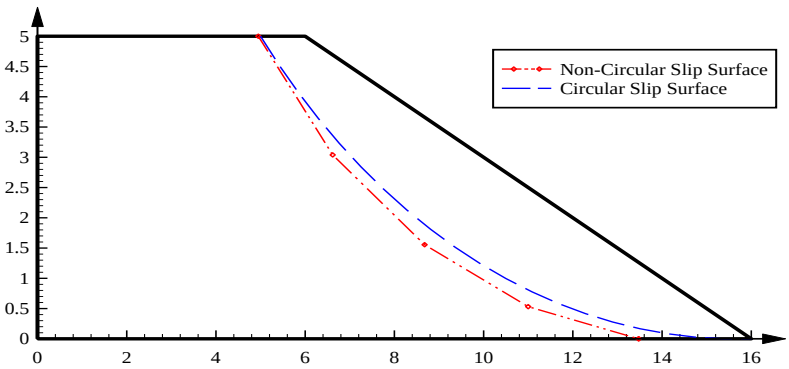

Figure 8. Comparison of initial and optimization slip surfaces with DOSS software for example 2 (this study)

Table 3: Geotechnical parameters for example 2

$\gamma(kN/m^3)$	φ (°)	$E(kN/m^2)$	$\vartheta(-)$
20.0	20.0	10^5	0.40

Table 4: Summary of factors of safety for example 2

Method	**Safety**	**FS** difference with

	Factor	Circular slip surface
LEM (Bishop/Geo-slope, Circular) [16]	1.376	
SRM [16]	1.387	-0.8
ELSM [16]	1.384	-0.6
AVLG(LEM-critical circular slip surface) [this study]	1.350	
AVLG(critical line-segments slip surface) [this study]	1.166	+13.6

4.3 Example 3

The third example is a slope with a weak layer (Fig. 9). The soil characteristics show in Table 5 for layers 1 to 4. Fig. 10 compares the critical slip surfaces obtained using the three methods by [16]. Two critical slip surfaces (circular and line-segments) of this work are shown in Fig. 11. As seen, the line-segments critical slip surface resulted from the AVLG method was similar to the slip surface obtained by [16] using SRM. According to Table 6, the improvement obtained for line-segment slip surface (19.7 %) using the AVLG method was higher than other methods (12.6%, 3.8% and 0.9%).

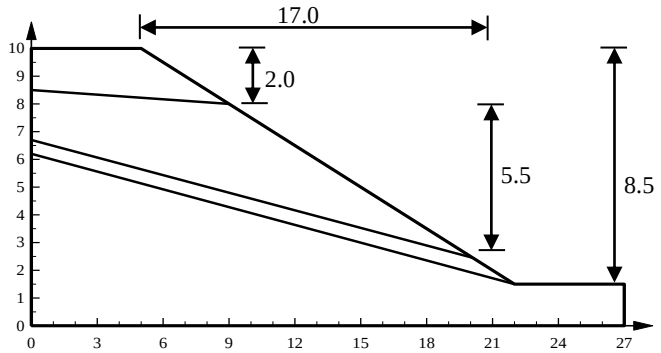

Figure 9. A slope in layered soil with a weak layer

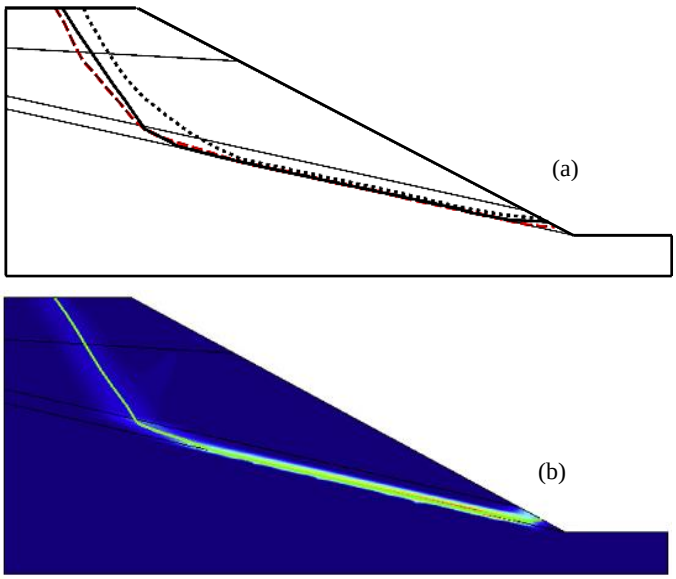

Figure 10. Comparisons of the critical slip surfaces obtained from (a) the LEM (solid line and dotted line) and ELSM (dashed line) and (b) the SRM [16]

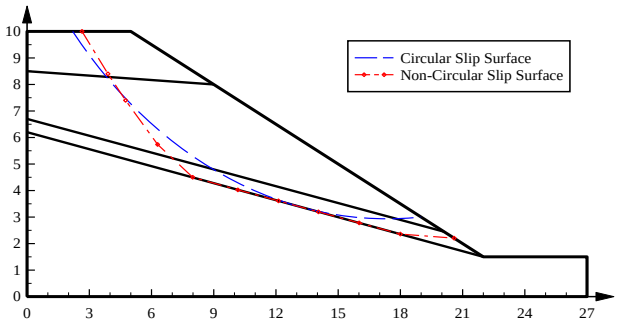

Figure 11. Comparison between initial and optimization slip surfaces using AVLG method for example 3 (this study)

Table 5: Geotechnical parameters for example 3

Layer	$\gamma(kN/m^3)$	$c\ (kPa)$	$\varphi\ (°)$	$E(kN/m^2)$	$\vartheta(-)$
1	18.62	15.0	20.0	10^5	0.35
2	18.62	17.0	21.0	10^5	0.35
3	18.62	5.0	10.0	10^5	0.35
4	18.62	35.0	28.0	10^5	0.35

Table 6: Summary of factors of safety for example 3

Method	**Safety Factor**	**FS** difference with Circular slip surface
LEM1 (M-P, Non-circular) [7]	1.240	12.6

LEM2 (Spencer, Non-circular) [7]	1.101	
SRM [16]	1.143	3.8
ELSM [16]	1.111	0.9
AVLG(LEM-critical circular slip surface)[this study]	1.424	
AVLG(critical line-segments slip surface)[this study]	1.143	19.7

4.4 Example 4

Fig. 12 shows a multi-stage slope. The unit weight, cohesion and internal angle of friction are $20\ \mathrm{kN/m^3}$, 5 kPa and 30° respectively. This example analyzed by [16]. The location of the critical slip surfaces and minimum FS analyzed by [16] are shown in Fig. 13. Fig. 14 shows the local and global line-segments slip surface obtained by the AVLG method. The locations and shapes of the local line-segments slip surface are similar to the results from [16]. Table 7 shows the values of FS obtained from different methods. As seen in this table, the FS of the critical circular slip surface obtained from AVLG is 1.325, which decreases to 1.296 for the line-segment critical slip surface.

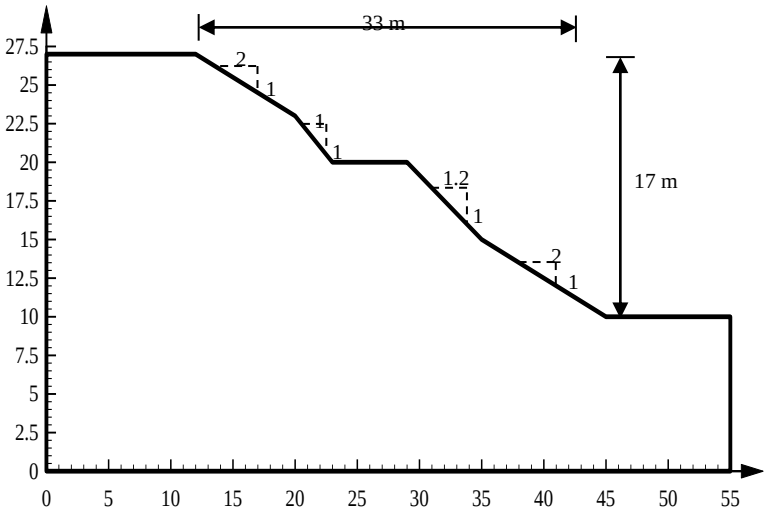

Figure 12. A multi-stage homogeneous slope where $E = 10^5\ kN/m^2$, $\upsilon = 0.49$, $\gamma = 20\ kN/m^3$, $\varphi = 30^{\circ}$, $c = 5\ kPa$

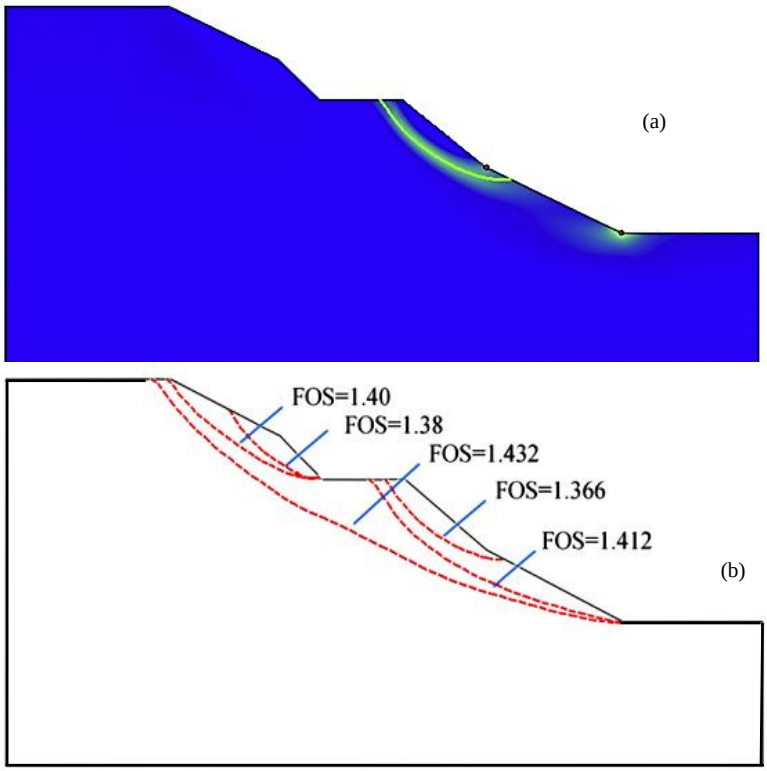

Figure 13. Comparisons of the slip surface: (a) critical slip surfaces obtained from the SRM and (b) critical failure surface from the ELSM [16]

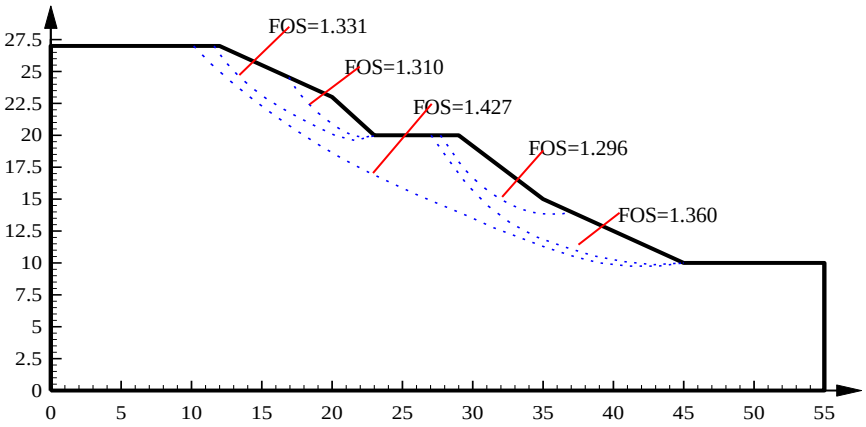

Figure 14. Line-segments critical slip surface and FS obtained from the AVLG method (this study)

Table 7: Summary of factors of safety for example 4

Method	**Safety Factor**	**FS** difference with Circular slip surface
LEM [16]	1.330	
SRM [16]	1.370	
ELSM [16]	1.366	
AVLG(LEM-critical circular slip surface)[this study]	1.325	
AVLG(critical line-segments slip surface)[this study]	1.296	+2.2

5. CONCLUSION

In this paper the line-segments slip surface is compared with circular and line-circular slip surface to show the line-segments slip surface is a flexible slip surface which has been addressed in this paper. The safety factor and the critical slip surfaces obtained by the LEM and two finite element methods (ELSM and SRM) are compared with the AVLG optimization method. The AVLG method has obtained line-segments critical slip surface but other methods have obtained circular or line-circular critical slip surface. The critical slip surfaces from the two finite element methods and the limit equilibrium method and AVLG method are in good agreement. The minimum safety factor from AVLG method is less than those from other methods. It be noted that the line-segments slip surface is more consistent with the actual slip surface in the nature and is more reliable and flexible than the others. The improvement obtained for critical line-segment slip surface with critical circular slip surface using 2D-AVLG was 19.7% in example 3 that it was higher than other methods.

REFERENCES

1. Bolton H. Heymann G, Groenwold A. Global search for critical failure surface in slope stability analysis, *Eng Optim* 2003; **35**(1): 51-65.
2. Jade S, Shanker KD. Modelling of slope failure using a global optimization technique, *Eng Optim* 1995; **23**(4): 255-66.
3. Arai K, Tagyo K. Determination of noncircular slip surface giving the minimum factor of safety in slope stability analysis, *Soil Foundat* 1985; **25**(1): 43-51.
4. Greco V. Efficient Monte Carlo technique for locating critical slip surface, *J Geotech Eng* 1996; **122**(7): 517-25.
5. Malkawi A, Hassan W, Sarma S. Global search method for locating general slip surface using Monte Carlo Techniques, *J Geotech Geoenviron Eng* 2001; **127**(8): 688-98.
6. Zolfaghari AR, Heath AC, Mccombie PF. Simple genetic algorithm search for critical non-circular failure surface in slope stability analysis, *Comput Geotech* 2005; **32**(3): 139-52.

7. Cheng YM, Li L, Chi SC, Wei WB. Particle swarm optimization algorithm for the location of the critical non-circular failure surface in two-dimensional slope stability analysis, *Comput Geotech* 2007; **34**(2): 92-103.
8. Rao SS. *Optimization Theory and Applications*, 2nd, Chapter 5, Wiley Eastern Limited, 1984.
9. Cheng YM. Locations of critical failure surface and some further studies on slope stability analysis, *Comput Geotech* 2003; **30**: 255-67.
10. Li KS, White W. Rapid evaluation of the critical slip surface in slope stability problems, *Int J Numer Analyt Method Geomech* 1987; **11**: 449-73.
11. Celestino, T.B. and Duncan, J.M. Simplified search for non-circular slip surfaces, *Proceedings of the 10th International Conference on Soil Mechanics and Foundation Engineering* 1981, International Society for Soil Mechanics and Foundation Engineering, Stockholm, 3. A.A. Balkema, Rotterdam, Holland, pp. 391-394.
12. Baker R. Determination of the critical slip surface in slope stability computations, *Int J Numer Analyt Method Geomech* 1980; **4**(4): 333-59.
13. Chun RH, Chameau JL. Three-dimensional limit equilibrium analysis of slopes, *Geotech* 1982; **32**(1): 31-40.
14. Chen Z, Shao C. Evaluation of minimum factor of safety in slope stability analysis, *Canadian Geotech J* 1983; **25**(4): 735-48.
15. Chen Z. Random trials used in determining global minimum factors of safety of slopes, *Canadian Geotech J* 1992; **29**(2): 225-33.
16. Liu SY, Shao LT, Li HJ. Slope stability analysis using the limit equilibrium method and two finite element methods, *Comput Geotech* 2015; **63**: 291-8.
17. Hajiazizi M, Tavana H. Determining three-dimensional non-spherical critical slip surface in earth slopes using an optimization method, *Eng Geology* 2013; **153**: 114-24.
18. Piña RJ, Jimenez R. Genetic algorithm for slope stability analyses with concave slip surfaces using custom operators, *Eng Optim* 2015; **47**(4): 453-72.
19. Kang F, Li J, Ma Z. An artificial bee colony algorithm for locating the critical slip surface in slope stability analysis, *Eng Optim* 2013, **45**(2): 207-23.
20. García-Palacios J, Castro C, Samartín, A. Optimal design in elasticity: a systematic adjoint approach to boundary cost functionals, *Optim Eng* 2015; **16**(4): 811-29.
21. Herzog R, Riedel I. Sequentially optimal sensor placement in thermoelastic models for real time applications, *Optim Eng* 2015; 16(4): 736-66.
22. Gheribi AE, Harvey JP, Bélisle E, Robelin C, Chartrand P, Pelton AD, Balel CW, Digabe SL. Use of a biobjective direct search algorithm in the process design of material science applications, *Optim Eng* 2016; **17**(1): 1-19.
23. Diouane Y, Gratton S, Vasseur X, Vicente LN, Calandra H. A parallel evolution strategy for an earth imaging problem in geophysics, *Optim Eng* 2016; **17**(1): 1-24.
24. DOSS program, Software of Determination of Optimal Slip Surface, Razi University, Iran, 2010.
25. Griffiths DV, Lane PA. Slope stability analysis by finite elements, *Géotech* 1999; **49**(3): 387-403.